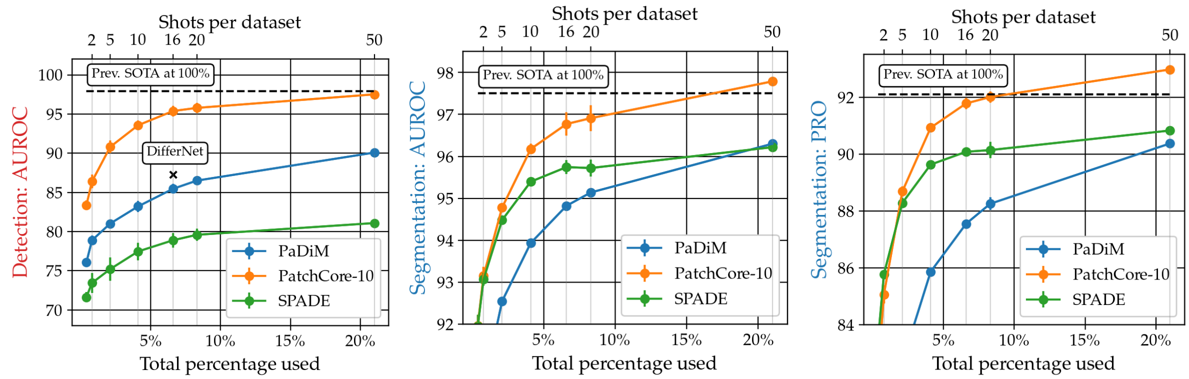

Figure 6. *PatchCore* shows notably higher sample-efficiency than competitors, matching the previous state-of-the-art with a fraction of nominal training data. Note that PaDiM and SPADE where reimplemented with WideResNet50 for comparability.

Table 6. Anomaly Segmentation on mSTC [32, 52] and anomaly detection on MTD [26] compared to results reported in [42].

mSTC	CAVGA-R_u [52]	SPADE [10]	PaDiM [14]	*PatchCore*−10
Pixelwise AUROC [%]	85	89.9	91.2	**91.8**
MTD	GANomaly [2]	1-NN [35]	DifferNet [42]	*PatchCore*−10
AUROC [%]	76.6	80.0	97.7	**97.9**

§C.1. As shown, using only one fifth of nominal training data, *PatchCore* can still match previous state-of-the-art performance. In addition, comparing to the 16-shot experiments performed in [42], we find *PatchCore* to outperform their approach which adapts a normalizing flows model on top of already pretrained features. Compared to image-level memory approaches in [10], we find matching localization and detection performance with only 5/1 nominal shots.

4.6. Evaluation on other benchmarks

We benchmark *PatchCore* on two additional anomaly detection performance benchmarks: The ShanghaiTech Campus dataset (STC) [32] and the Magnetic Tile Defects dataset (MTD) [26]. Evaluation for STC as described in §4.1 follows [52], [14] and [10]. We report unsupervised anomaly localization performance on a subsampled version of the STC video data (mSTC), with images resized to 256×256 [14]. As the detection context is much closer to natural image data available in ImageNet, we make use of deeper network feature maps at hierarchy levels 3 and 4, but otherwise do not perform any hyperparameter tuning for *PatchCore*. The results in Table 6 (*top*) show state-of-the-art anomaly localization performance which suggests good transferability of *PatchCore* to such domains. Finally, we examine MTD, containing magnetic tile defect images of varying sizes on which spatially rigid approaches like PaDiM cannot be applied directly. Here, nominal data already exhibits high variability similar to those encountered in anomalous samples [42]. We follow the protocol proposed in [42] to measure image-level anomaly detection performance and find performance to match (and even slightly outperform) that of [42] (Table 6, *bottom*).

5. Conclusion

This paper introduced the *PatchCore* algorithm for cold-start anomaly detection, in which knowledge of only nominal examples has to be leveraged to detect and segment anomalous data at test-time. *PatchCore* strikes a balance between retaining a maximum amount of nominal context at test-time through the usage of memory banks comprising locally aware, nominal patch-level feature representations extracted from ImageNet pretrained networks, and minimal runtime through coreset subsampling. The result is a state-of-the-art cold-start image anomaly detection and localization system with low computational cost on industrial anomaly detection benchmarks. On MVTec, we achieve an image anomaly detection AUROC over 99% with highest sample efficiency in relevant small training set regimes.

Broader Impact. As automated industrial anomaly detection is one of the most successful applications of Computer Vision, the improvements gained through *PatchCore* can be of notable interest for practitioners in this domain. As our work focuses specifically on industrial anomaly detection, negative societal impact is limited. And while the fundamental approach can potentially we leveraged for detection systems in more controversial domains, we don't believe that our improvements are significant enough to change societal application of such systems.

Limitations. While *PatchCore* shows high effectiveness for industrial anomaly detection without the need to specifically adapt to the problem domain at hand, applicability is generally limited by the transferability of the pretrained features leveraged. This can be addressed by merging the effectiveness of *PatchCore* with adaptation of the utilized features. We leave this interesting extension to future work.